IEEE Access
Multidisciplinary | Rapid Review | Open Access Journal

Received October 4, 2020, accepted October 29, 2020, date of publication November 5, 2020, date of current version November 17, 2020.

Digital Object Identifier 10.1109/ACCESS.2020.3036092

Stochastic Economic Dispatching Strategy of the Active Distribution Network Based on Comprehensive Typical Scenario Set

HUIMIN ZHU, (Student Member, IEEE), SHUN YUAN, (Member, IEEE), AND CHUNLAI LI, (Member, IEEE)
School of Electrical Engineering, Shenyang University of Technology, Shenyang 110870, China
Corresponding author: Huimin Zhu (759066795@qq.com)

This work was supported by the Science and Technology Project of State Grid Corporation of China under Grant 2017-0-32-2-10.

ABSTRACT The increasing penetration of renewable energy resources in the distribution network has posed great uncertainties and challenges for the system security operation. To model various uncertain factors like the wholesale market price and renewable energy generation in the active distribution network (ADN), a similarity measurement method considering the amplitude, volatility and variation trend is proposed. The Latin hypercube sampling method and Graph Pyramid clustering algorithm are adopted to obtain the comprehensive typical scenario set. Furthermore, this study proposes a scenario-based stochastic day-ahead optimal economic dispatch approach based on typical scenario set. The energy trading between the distribution system and the wholesale energy market, various distributed generators, network topology and power flow model are jointly formulated in the proposed operation model. The effectiveness and scalability of the proposed approach are verified using the IEEE 33-bus system. Numerical simulation results under different implementation scenarios indicate that the proposed approach offers a high computational efficiency and promotes the security and economy of the distribution system operation, which has a promising industrial application value.

INDEX TERMS Active distribution network, renewable energy resources, stochastic optimization, clustering algorithm, typical scenario set.

I. INTRODUCTION

With the increasing renewable energy generation in the distribution network, the structure of distribution network tends to be complex, and its control and operation will face significant challenges [1], [2]. Unlike the transmission network, the line resistance of the active distribution network cannot be ignored. To take the voltage and reactive power into account, the calculation of optimal power flow must be based on the AC power flow constraints [3]. Mathematically, the calculation of optimal power flow of active distribution network is a mixed integer non-convex programming problem [4], [5].

The research on the optimal power flow of active distribution network with multiple uncontrollable sources is very limited. However, if the output of the distributed generation is fixed, the optimal power flow of the active distribution network with multiple uncontrollable sources is an intractable problems. There are three kinds of common methods to solve this problem. The first is the continuous regularization algorithm, which first relaxes the discrete variables to continuous variables, and then regularizes the variables in order. In [6], a optimization method based on interior point method and Gaussian penalty function is proposed to cope with large-scale reactive power flow optimization. Reference [7] proposes a two-stage dynamic reactive power optimization algorithm based on heuristic search and variable correction. The second category of solution adopts nonlinear primal dual algorithm. Reference [8] proposes a reactive power optimization algorithm with penalty function embedded in nonlinear primal dual interior point method. Reference [8] and [9] construct penalty functions for discrete variables and realize the successive integration of discrete variables in the optimization process. A new algorithm using the primal dual interior point method with the predictor-corrector for solving

The associate editor coordinating the review of this manuscript and approving it for publication was Sudhakar Babu Thanikanti.

nonlinear optimal power flow problems is also presented in [10]. To guarantee the voltage stability, [11] integrates branch-bound method and primal dual interior point method to dynamic optimal power flow problem. The third category of method are heuristic algorithms, including genetic algorithm [12],[13], particle swarm optimization [14],[15], etc. Moreover, the reinforcement learning and deep learning approaches are promising techniques for model free or non-convex stochastic optimization problems [16], [17]. Besides, the machine learning approach is a promising technique to improve the forecasting accuracy and reduce the system uncertainties [18].

In recent years, the method of solving optimal power flow based on convex relaxation has been widely applied [19]. Especially, a novel method based on second-order cone relaxation is provided to optimize power flow. This method is based on the branch power flow model. By relaxing the quadratic equality constraint to the second-order cone constraint, the original non-convex and nonlinear problem can be transformed into an efficient second-order cone optimization problem. Considering the mixed integer second-order cone programming is also mature, it provides a feasible way to solve the optimal power flow problem of active distribution network with discrete variables [20]. In the power market, there are many random factors in the distribution system (including the electricity price, load demand, photovoltaic, wind power and other kinds of distributed resources), which bring challenges to the power system scheduling and control [21]. At present, the spinning reserve of conventional generators is used to deal with the uncertainty of renewable energy in actual operation of the power grid [22]. Robust optimization methods [23],[24] and stochastic optimization methods [25], [26] are commonly used methods to cope with the uncertainty.

Robust optimization uses uncertain parameter interval to describe the uncertainty. The optimal results can be obtained under the condition that all uncertain variables meet all constraints in their feasible ranges. In [27], robust real-time dispatch is formulated as an adjustable robust optimization model incorporating an adjustable controlling strategy compatible with AGC systems. The proposed model can be equivalently transformed to a nonlinear programming problem with linear constraints via duality. [28] proposes a robust stochastic optimization model to handle the uncertainty of wind power in dynamic economic dispatch. [29] describes a robust optimization model for wind power accommodation. The model calculates allowable interval solutions for wind power generation and provides optimal economic solutions for conventional power generation to mitigate the uncertainty inherent to wind power. The disadvantage of robust optimization is that it focuses on describing the extreme situation in the optimization process, and the economic efficiency of optimization results is poor.

The stochastic optimization approach are mainly divided into chance constraint based method [30] and scenario set method [31]–[35]. The stochastic optimization approach based on scenario set is not limited by the model types and is widely used in formulating the uncertainties in the power systems, which includes the following two steps [31], [32]: Firstly, the typical scenario set is obtained by scenario sampling and reduction, and then the model is optimized based on multiple typical scenarios to obtain the expected optimal value. This method can fully consider the uncertainty of many factors at the same time, and the optimization results are more close to the actual situation. *Yi et al.* [33] first utilize the typical scenario set into the virtual power plant management considering a large number of deferrable loads. Reference [34] proposes an innovative probabilistic clustering concept for aggregate modeling of wind farms. The proposed technique determines the number of equivalent turbines that can be used to represent large wind farms during the year in system studies. The self-organizing map clustering algorithm is used in [35] to identify the fluctuation categories of wind power.

In view of this, based on the comprehensive typical scenario set, this study proposes a stochastic economic dispatching strategy for the active distribution network. The major contributions of this study are summarized into the following threefold:

(1). Based on the Latin hypercube sampling approach [36] and Graph Pyramid clustering method [38], a novel typical scenario set consisting of various uncertain factors is formulated in this study. It is more suitable for application to the actual operation with high requirement for computation efficiency.

(2). Compared with the traditional scenario reduction methods that mainly focus on the amplitude in [31]-[33], the proposed scenario reduction methods can comprehensively measure the differences among different scenarios in terms of amplitude, volatility and variation trend, which makes the obtained typical scenario set more reasonable.

(3). In addition to modeling the controllable units and system security operation constraints, the interaction between the distribution network and superior wholesale energy market is formulated in the proposed stochastic ADN day-ahead economic dispatching strategy, which can enable the distribution system operators (DSO) to perform as a prosumer when participating in the wholesale market operation.

The rest of this study is organized as follows. Section II presents the generation and reduction method of the comprehensive typical scenario set. Section III proposes an optimal energy management approach based on the typical scenario set. Section IV presents case studies on IEEE 33-bus distribution system. Section V concludes this study.

II. GENERATION AND REDUCTION METHOD OF TYPICAL SCENARIO SET

A. SCENARIO GENERATION BASED ON LATIN HYPERCUBE SAMPLING

Under power market background, there are many uncertain factors in the distribution network, such as the wind power

generation forecasting, photovoltaic generation forecasting, wholesale market price and so on. According to the probability density distribution of all kinds of random factors, the Latin hypercube sampling method is adopted here to sample all kinds of factors and get a large number of random scenarios. Latin hypercube sampling has the characteristics of high sampling efficiency. It can fully maintain the original probability distribution of various random factors [36]. The detailed implementation steps are as follows:

Step 1: According to the probability distribution of each random factor, it is divided into NL intervals of equal probability;

Step 2: For probability interval $[\frac{i-1}{NL}, \frac{i}{NL}]$, $i = 1,2,\ldots, NL$, select a number s_i from this interval randomly. The selection method is as follows:

$$s_i = \frac{num}{NL} + \frac{i-1}{NL} \tag{1}$$

where num is a random number in [0,1].

Step3: Based on the inverse transformation of probability density distribution, the corresponding sample parameters can be obtained

$$x_i = F^{-1}(s_i) \tag{2}$$

where x_i is the sample value, $F^{-1}(\cdot)$ is the inverse function of probability distribution.

According to the above steps, all kinds of random factors are sampled separately to obtain a large number of random scenarios including the wind power, photovoltaic, wholesale market price.

B. COMPREHENSIVE SIMILARITY MEASUREMENT

In this subsection, the similarities of the uncertain factors in different scenarios are measured in terms of multiple scales including the amplitude, volatility and variation trend of random factors.

Firstly, all the random factors should be normalized.

$$\tilde{x}_i^R(t) = \frac{x_i^R(t) - \min\limits_{R\in \boldsymbol{RN}, i\in \boldsymbol{SN}}\left[x_i^R(t)\right]}{\max\limits_{R\in \boldsymbol{RN}, i\in \boldsymbol{SN}}\left[x_i^R(t)\right] - \min\limits_{R\in \boldsymbol{RN}, i\in \boldsymbol{SN}}\left[x_i^R(t)\right]} \tag{3}$$

where $x_i^R(t)$ is the value of random factor R at time t in scenario i. $\tilde{x}_i^R(t)$ is the normalized value of random factor R at time t in scenario i. $\boldsymbol{RN}$ is the set of random factors. $\boldsymbol{SN}$ is the set of scenarios.

1) MEASUREMENT OF AMPLITUDE DIFFERENCE

Euclidean distance is adopted to describe the amplitude difference of random factor R in different scenarios. The greater the Euclidean distance represents smaller similarity.

$$A^R(i,j) = \sqrt{\sum_{t=1}^{T}\left[\tilde{x}_i^R(t) - \tilde{x}_j^R(t)\right]^2} \tag{4}$$

where $A^R(i,j)$ is the amplitude difference of random factor R between scenario i and scenario j. T is the number of time points generated by sampling.

2) MEASUREMENT OF SIMILARITY OF THE VOLATILITY

The similarity of the volatility of random factors is measured using relative distance in different scenarios. The relative distance between $\tilde{x}_i^R(t)$ and $\tilde{x}_j^R(t)$ is as follows:

$$F^R(i,j) = \frac{1}{T}\sum_{t=1}^{T}\left|\tilde{x}_i^R(t) - \tilde{x}_j^R(t)\right| \tag{5}$$

where $F^R(i,j)$ is the difference matrix of fluctuation degree between scenario i and scenario j.

3) MEASUREMENT OF VARIATION TREND

Correlation coefficient is used to represent the difference of variation trend of random factor R in different scenarios.

$$C^R(i,j) = 1 - \frac{\sum\limits_{t=1}^{T}\left[\tilde{x}_i^R(t) - \bar{x}_i^R\right]\cdot\left[\tilde{x}_j^R(t) - \bar{x}_j^R\right]}{\sqrt{\sum\limits_{t=1}^{T}\left[\tilde{x}_i^R(t) - \bar{x}_i^R\right]^2}\cdot\sqrt{\sum\limits_{t=1}^{T}\left[\tilde{x}_j^R(t) - \bar{x}_j^R\right]^2}} \tag{6}$$

where $\bar{x}_i^R$ is the average value of random factor R in scenario i; $C^R(i,j)$ is the difference matrix of of variation trend between scenario i and scenario j.

According to the similarity measurement described above, the comprehensive difference matrix $\boldsymbol{P}$ can be calculated by considering the amplitude, volatility and variation trend of random factors.

$$\boldsymbol{P} = \sum_{R=1}^{RN}\left(\alpha\cdot\tilde{\boldsymbol{A}}^R + \beta\cdot\tilde{\boldsymbol{F}}^R + \gamma\cdot\tilde{\boldsymbol{C}}^R\right) \tag{7}$$

where $\tilde{\boldsymbol{A}}^R, \tilde{\boldsymbol{F}}^R, \tilde{\boldsymbol{C}}^R$ are normalized matrix of $\boldsymbol{A}^R, \boldsymbol{F}^R, \boldsymbol{C}^R$, respectively. α, β, γ are weight coefficient.

Gaussian kernel function is an effective method to describe the comprehensive difference among different scenarios. The above multi-scale difference matrix can be transformed into comprehensive similarity measurement matrix by applying Gaussian kernel function.

$$G(i,j) = \exp\left\{-\frac{[P(i,j)]^2}{2\cdot wid^2}\right\} \tag{8}$$

where wid is the width parameter of Gaussian kernel function. $G(i,j)$ is the similarity between scenario i and scenario j. $\boldsymbol{G}$ is the similarity matrix and its value of elements within [0,1]. The larger $G(i,j)$ is, the higher the similarity between scenario i and scenario j. The elements on the diagonal of $\boldsymbol{G}$ matrix are 1, which means that the two scenarios are identical. The determination of width parameter wid can refer to [37].

C. SCENARIO REDUCTION BASED ON GRAPH PYRAMID CLUSTERING ALGORITHM

1) BUILD MINIMUM SPANNING TREE

To achieve multi-resolution based clustering, data points can be represented as a minimum spanning tree (MST) [38]. The information of node density and its adjacent nodes can be

obtained from MST. Given a dataset $\boldsymbol{D}$ with n data points and data points can be regarded as n nodes in MST. The weight of the edge in MST is equal to the Euclidean distance between the corresponding two data points. The MST is a spanning tree with the least weight sum of n-1 edges.

2) CALCULATION OF NODE PRIORITY

After MST is constructed by all data points in the dataset, the next step is to traverse each node and merge some nodes that are close to each other. It will result in wrong clustering results if the nodes are traversed in order. As shown in Fig. 1, the ideal merging scheme is to merge nodes 1 and 2, and merge nodes 3, 4 and 5. However, if node 3 is found first during traversal, it is very likely that neighboring nodes 2, 4, 5 will be merged with node 3, while the closer nodes 1, 2 will not be merged.

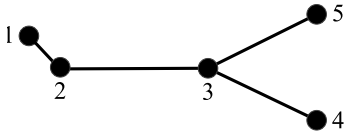

FIGURE 1. Schematic diagram of data points.

In order to get the correct clustering results, the nodes should be traversed based on priority. The nodes with higher density should have higher priority, so that they can merge the neighboring nodes. The degree of node in MST is proportional to its density.

When defining the priority of a node, the following principles should be followed:

(a) The greater the degree of the node, the higher the priority;

(b) If some nodes have same degree, the shorter the length of the shortest edge connected to the node, the higher the priority of the node should be.

According to the above principles, we define the priority pri_n of node n as follows:

$$pri_n = wei \times d_{norm}(n) + (1 - wei) \times e^{\min}_{norm}(n). \quad (9)$$

$$d_{norm}(n) = \frac{d(n) - 1}{D_{\max} - 1 + \varepsilon}. \quad (10)$$

$$e^{\min}_{norm}(n) = \frac{E_{\max} - e^{\min}(n)}{E_{\max} - E_{\min} + \varepsilon} \quad (11)$$

where $wei \in (0, 1)$ is the weight factor. $d_{norm}(n)$ is the normalization degree of node n. It can be calculated by the degree $d(n)$ of node n, the maximum degree D_{max} in the MST, and a small constant value ε. $e^{min}_{norm}(n)$ is the normalized length of the shortest edge of node n. $e^{min}(n)$ represents the shortest edge length connecting to node n. E_{max}/E_{min} are the longest edge and the shortest edge of MST respectively. ε is used to avoid the denominator is equal to zero in Equation (10) and (11).

3) NODE TRAVERSAL AND MERGING

Traverse all nodes in MST in descending order of priority, and judge whether the traversed node n has ever been merged. If node n has participated in the merge, it is no longer allowed to participate in the merge. Otherwise, all nodes connecting to node n should be found in MST. Then, select the node with the shortest edge from node n and merge them together. Suppose that there are N_{node} nodes need to be merged: $v_1 = \{a_{11}, a_{12}, \ldots, a_{1l}\}$, $v_2 = \{a_{21}, a_{22}, \ldots, a_{2l}\}, \ldots, v_{N_{node}} = \{a_{N_{node}1}, a_{N_{node}2}, \ldots, a_{N_{node}L}\}$. L represents the number of node attributes. The new node after merging is represented as $\bar{v} = \{\bar{a}_1, \bar{a}_2, \ldots, \bar{a}_l$ and its attributes can be calculated as follows:

$$\bar{a}_n = \sum_{l=1}^{N_{node}} \frac{m_l}{M} a_{ln} \quad (12)$$

where M is the total mass of N_{node} nodes. m_l represents the mass of original node l.

The whole algorithm flow is shown in Fig. 2.

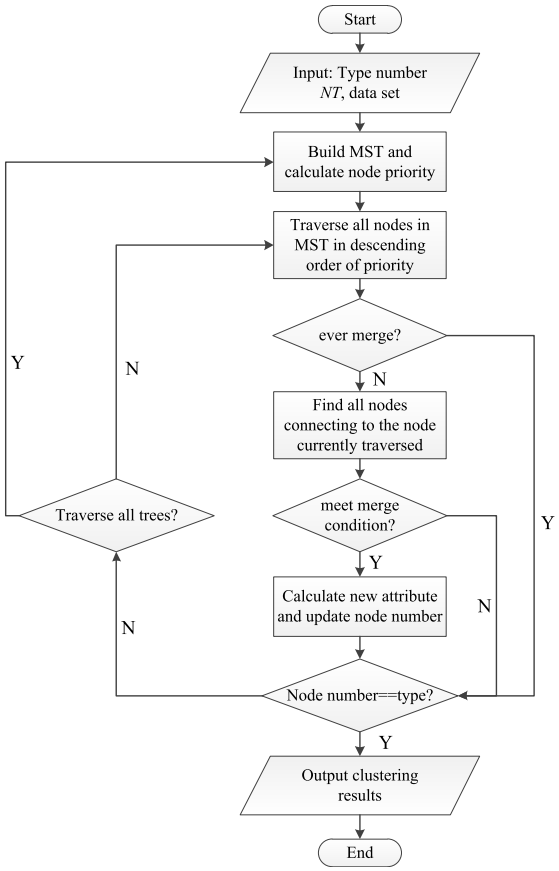

FIGURE 2. Algorithm flow chart of node traversal and merging.

Assume that the initial mass of all nodes in MST is 1. The mass of the new node is equal to the sum of the mass of all nodes, which is actually the total number of nodes participating in the merge. According to (12), the greater the mass of the nodes participating in the merger is, the greater

the weight in the attribute value. It means that the new node is closer to the original node. The traversal is ended when all N_{node} nodes are traversed or N_{node} is equal to the class number NT. If the current total number of nodes is greater than the category number NT, MST will be generated for the current node, and continue to traverse all new nodes. If the current total number of nodes is equal to the category number NT, these NT nodes are the clustering results.

III. OPTIMAL ENERGY MANAGEMENT APPROACH BASED ON TYPICAL SCENARIO SET

A. OBJECTIVE FUNCTION

The optimal dispatch model of distribution system operators (DSO) aims to minimize the operation cost of distribution system. The operation cost of distribution system is equal to the sum of the energy purchasing cost from the wholesale market of the transmission level, the operation cost of the internal controllable resources and the curtailment cost of renewable energy generation in distribution network. The output of optimal dispatch model includes the hourly energy bidding plan provided to the wholesale market, and the dispatching plan used to control devices. The objective function is as follows:

$$\begin{aligned}\min_{x} \quad & \sum_{s=1}^{N_s}\{w_s \cdot \sum_{t=1}^{T}[\pi_{\mathrm{DN},s,t} \cdot \hat{P}^{\mathrm{BP}}_{\mathrm{DN},s,t} \\ & + \sum_{i=1}^{N_{\mathrm{CG}}} F_i^{\mathrm{CG}}(\hat{P}^{\mathrm{CG}}_{s,i,t}) + \sum_{i=1}^{N_{\mathrm{PV}}} F_i^{\mathrm{PV}}(\hat{P}^{\mathrm{PV}}_{s,i,t}) \\ & + \sum_{i=1}^{N_{\mathrm{WF}}} F_i^{\mathrm{WF}}(\hat{P}^{\mathrm{WF}}_{s,i,t}) + \sum_{k=1}^{N_{ESS}} F_i^{ESS}(\hat{P}^{ESS,in}_{s,i,t}, \hat{P}^{ESS,out}_{s,i,t})]\} \end{aligned} \quad (13)$$

where N_S is the number of typical scenarios. w_s is the weight coefficient of each scenario. $N_{CG}, N_{pv}, N_{WF}, N_{ESS}$ are number of controllable units, photovoltaic systems, wind farm, and energy storage system, respectively. $\pi_{DN,s,t}$ is the unit cost of purchasing power from wholesale market. $\hat{P}^{BP}_{DN,s,t}$ is the amount of electricity purchased from wholesale market at time t in scenario s. $F_i^{CG}(\hat{P}^{CG}_{s,i,t})$ and $F_i^{ESS}(\hat{P}^{ESS,in}_{s,i,t}, \hat{P}^{ESS,out}_{s,i,t})$ are cost functions of controllable generating units and energy storage systems, respectively. $F_i^{PV}(\hat{P}^{PV}_{s,i,t})$ and $F_i^{WF}(\hat{P}^{WF}_{s,i,t})$ represents the curtailment cost of photovoltaic systems and wind farms. $\hat{P}^{CG}_{s,i,t}$, $\hat{P}^{PV}_{s,i,t}$, $\hat{P}^{WF}_{s,i,t}$, $\hat{P}^{ESS,out}_{s,i,t}$ are output of controllable generating unit, photovoltaic system, wind farm, and energy storage system at time t in scenario s. $\hat{P}^{ESS,in}_{s,i,t}$ is the charging power of energy storage system i at time t in scenario s.

The decision variables of the economic problem are summarized as: $x = \{\hat{P}^{\mathrm{BP}}_{\mathrm{DN},s,t}, \hat{P}^{\mathrm{CG}}_{s,i,t}, \hat{P}^{\mathrm{PV}}_{s,i,t}, \hat{P}^{\mathrm{WF}}_{s,i,t}, \hat{P}^{\mathrm{PV}}_{s,i,t}, \hat{P}^{\mathrm{WF}}_{s,i,t}, \hat{P}^{ESS,in}_{s,i,t}, \hat{P}^{ESS,out}_{s,i,t}\}$.

The operation cost of the controllable generators and energy storage system can be expressed as

$$F_i^{\mathrm{CG}}(\hat{P}^{\mathrm{CG}}_{s,i,t}) = a_i \cdot (\hat{P}^{\mathrm{CG}}_{s,i,t})^2 + b_i \cdot \hat{P}^{\mathrm{CG}}_{s,i,t} + c_i. \quad (14)$$

$$F_i^{ESS}(\hat{P}^{ESS,in}_{s,i,t}, \hat{P}^{ESS,out}_{s,i,t}) = inc_i \cdot \hat{P}^{ESS,in}_{s,i,t} + outc_i \cdot \hat{P}^{ESS,out}_{s,i,t} \quad (15)$$

where a_i, b_i, c_i are cost coefficients of unit i. inc_i and $outc_i$ are cost coefficients of charging and discharging power of energy storage system i. The curtailment cost functions of RESs are given as:

$$F_i^{PV}(\hat{P}^{PV}_{s,i,t}) = Ab_i^{PV} \cdot \left(\hat{P}^{PV,fore}_{s,i,t} - \hat{P}^{PV}_{s,i,t}\right)^2. \quad (16)$$

$$F_i^{WF}(\hat{P}^{WF}_{s,i,t}) = Ab_i^{WF} \cdot \left(\hat{P}^{WF,fore}_{s,i,t} - \hat{P}^{WF}_{s,i,t}\right)^2 \quad (17)$$

where Ab_i^{PV}/Ab_i^{WF} are curtailment cost coefficients of photovoltaic system i and wind farm i, respectively. $\hat{P}^{PV,fore}_{s,i,t}/\hat{P}^{WF,fore}_{s,i,t}$ are forecasted outputs of photovoltaic system i and wind farm i at time t in scenario s, respectively.

B. SECURITY CONSTRAINTS OF CONTROLLABLE DEVICES

The security constraints of generating units, renewable energy systems, wind farms and energy storage systems can be summarized as follows:

$$-\hat{P}^{\mathrm{CG}}_{s,i,\min} \le \hat{P}^{\mathrm{CG}}_{s,i,t} \le \hat{P}^{\mathrm{CG}}_{s,i,\max}. \quad (18)$$

$$-\Delta\hat{P}^{\mathrm{CG}}_{s,i} \le \hat{P}^{\mathrm{CG}}_{s,i,t} - \hat{P}^{\mathrm{CG}}_{s,i,t-1} \le \Delta\hat{P}^{\mathrm{CG}}_{s,i}. \quad (19)$$

$$0 \le \hat{P}^{PV}_{s,i,t} \le \hat{P}^{PV,fore}_{s,i,t}. \quad (20)$$

$$0 \le \hat{P}^{WF}_{s,i,t} \le \hat{P}^{WF,fore}_{s,i,t}. \quad (21)$$

$$\begin{aligned}\hat{E}^{ESS}_{s,i,t+1} = \hat{E}^{ESS}_{s,i,t} + \Delta t \cdot \Big(\hat{P}^{ESS,in}_{s,i,t} \\ \cdot\eta_1^{ESS} - \hat{P}^{ESS,out}_{s,i,t}/\eta_2^{ESS}\Big).\end{aligned} \quad (22)$$

$$\hat{E}^{ESS}_{s,i,\min} \le \hat{E}^{ESS}_{s,i,t} \le \hat{E}^{ESS}_{s,i,\max}. \quad (23)$$

$$0 \le \hat{P}^{ESS,in}_{s,i,t} \le sta^{in}_{s,i,t} \cdot \hat{P}^{ESS,in}_{s,i,t}. \quad (24)$$

$$0 \le \hat{P}^{ESS,out}_{s,i,t} \le sta^{out}_{s,i,t} \cdot \hat{P}^{ESS,out}_{s,i,t}. \quad (25)$$

$$0 \le sta^{in}_{s,i,t} + sta^{out}_{s,i,t} \le 1. \quad (26)$$

where $\hat{P}^{CG}_{s,i,min}/\hat{P}^{CG}_{s,i,max}$ are minimum and maximum output of generating unit i in scenario s. $\Delta\hat{P}^{CG}_{s,i}$ is the ramp rate limitation of generating unit i in scenario s. $\hat{E}^{ESS}_{s,i,t}$ is the energy level of energy storage system i at time t in scenario s. $\hat{E}^{ESS}_{s,i,min}/\hat{E}^{ESS}_{s,i,max}$ are minimum and maximum energy level of energy storage system i in scenario s. $\eta_1^{ESS}/\eta_2^{ESS}$ are efficiencies of charging and discharging process, respectively. $sta^{in}_{s,i,t}/sta^{out}_{s,i,t}$ are binary variables to represent charging and discharging working states. Equations (18)-(19) represent the operation constraints of generating units. Equations (20)-(21) are operation constraints of photovoltaic systems and wind farms. Equations (22)-(26) describes the security constraints of energy storage systems.

When the optimal solution is obtained, $\hat{P}^{ESS,in}_{s,i,t}$ and $\hat{P}^{ESS,out}_{s,i,t}$ cannot be positive simultaneously and the binary variables $sta^{in}_{s,i,t}/sta^{out}_{s,i,t}$ in (26) can be dropped [39]. Suppose that $\bar{P}^{ESS,in}_{s,i,t}$ and $\bar{P}^{ESS,out}_{s,i,t}$ are positive and $\bar{P}^{ESS,in}_{s,i,t} - \bar{P}^{ESS,out}_{s,i,t} = K > 0$. There always exists another solution where $\hat{P}^{ESS,in}_{s,i,t} = K$ and $\hat{P}^{ESS,out}_{s,i,t} = 0$. Their corresponding objective function values are $\bar{f}$ and $\hat{f}$, respectively. It is easy to show that $\hat{P}^{ESS,in}_{s,i,t}$ and $\hat{P}^{ESS,out}_{s,i,t}$ also satisfy (22)-(26) and $\bar{f} > \hat{f}$.

Hence, $\hat{P}^{ESS,in}_{s,i,t}$ and $\hat{P}^{ESS,out}_{s,i,t}$ are the optimal solution rather than $\bar{P}^{ESS,in}_{s,i,t}$ and $\bar{P}^{ESS,out}_{s,i,t}$.

C. SYSTEM SECURITY CONSTRAINTS

To guarantee the security operation of distribution power system, the following constraints should be satisfied.

$$\sum_{i=1}^{N_{\mathrm{CG}}} \hat{P}^{\mathrm{CG}}_{i,\max} - \sum_{i=1}^{N_{\mathrm{CG}}} \hat{P}^{\mathrm{CG}}_{i,t} \geq \sum_{i=1}^{N_{\mathrm{L}}} \left|\Delta \hat{P}^{\mathrm{L}}_{s,i,t}\right| + \sum_{i=1}^{N_{\mathrm{WF}}} \left|\Delta \hat{P}^{\mathrm{WF}}_{s,i,t}\right| + \sum_{i=1}^{N_{\mathrm{PV}}} \left|\Delta \hat{P}^{\mathrm{PV}}_{s,i,t}\right|. \tag{27}$$

$$\sum_{i=1}^{N_{\mathrm{CG}}} \hat{P}^{\mathrm{CG}}_{i,t} - \sum_{i=1}^{N_{\mathrm{CG}}} \hat{P}^{\mathrm{CG}}_{i,\min} \geq \sum_{i=1}^{N_{\mathrm{L}}} \left|\Delta \hat{P}^{\mathrm{L}}_{s,i,t}\right| + \sum_{i=1}^{N_{\mathrm{WF}}} \left|\Delta \hat{P}^{\mathrm{WF}}_{s,i,t}\right| + \sum_{i=1}^{N_{\mathrm{PV}}} \left|\Delta \hat{P}^{\mathrm{PV}}_{s,i,t}\right|. \tag{28}$$

$$\begin{cases} P_i = \hat{P}^{\mathrm{BP}}_{\mathrm{DN},s,t} + \hat{P}^{\mathrm{CG}}_{s,i,t} + \hat{P}^{\mathrm{PV}}_{s,i,t} + \hat{P}^{\mathrm{WF}}_{s,i,t} - \hat{P}^{\mathrm{L}}_{s,i,t} \\ Q_i = \hat{Q}^{\mathrm{G}}_{i,t} - \hat{Q}^{\mathrm{L}}_{i,t}. \end{cases} \tag{29}$$

$$\sum_{i\in\Omega_{i\to j}} (P_{ij} - \frac{P_{ij}^2 + Q_{ij}^2}{V_i^2} r_{ij}) + P_j - g_j V_j^2 = \sum_{k\in\Omega_{j\to k}} P_{jk}. \tag{30}$$

$$\sum_{i\in\Omega_{i\to j}} (Q_{ij} - \frac{P_{ij}^2 + Q_{ij}^2}{V_i^2} x_{ij}) + Q_j - b_j V_j^2 = \sum_{k\in\Omega_{j\to k}} Q_{jk}. \tag{31}$$

$$V_j^2 = V_i^2 - 2(r_{ij}P_{ij} + x_{ij}Q_{ij}) + (r_{ij}^2 + x_{ij}^2)\frac{P_{ij}^2 + Q_{ij}^2}{V_i^2}. \tag{32}$$

$$V_{i,\min} \leq V_i \leq V_{i,\max}. \tag{33}$$

$$P_{ij,\min} \leq P_{ij} \leq P_{ij,\max}. \tag{34}$$

$$Q_{ij,\min} \leq Q_{ij} \leq Q_{ij,\max}. \tag{35}$$

$$-\hat{P}^{\mathrm{BP}}_{\mathrm{DN},s,\max} \leq \hat{P}^{\mathrm{BP}}_{\mathrm{DN},s,t} \leq \hat{P}^{\mathrm{BP}}_{\mathrm{DN},s,\max}. \tag{36}$$

where $\hat{P}^{BP}_{DN,s,min}/\hat{P}^{BP}_{DN,s,max}$ are the minimum and maximum purchasing power from the wholesale market. $\Delta\hat{P}^{L}_{s,i,t}$, $\Delta\hat{P}^{WF}_{s,i,t}$, $\Delta\hat{P}^{PV}_{s,i,t}$ represent predict errors of power load, wind farm, photovoltaic system i at time t in scenario s. $\hat{P}^{L}_{s,i,t}$, $\hat{Q}^{G}_{i,t}$, $\hat{Q}^{L}_{i,t}$ are active power load, reactive power output, and reactive power load. r_{ij} and x_{ij} are the resistance and reactance of the line between bus i and bus j. g_i and b_i are the conductance and susceptance to the earth of bus j. $P_{ij,min}/P_{ij,max}$ are the lower and upper limit of active power flow of branch ij. $Q_{ij,min}/Q_{ij,max}$ are the lower and upper limit of reactive power flow of branch ij. $\Omega_{i\to j}$ represent the sets of the power flowing from bus i to bus j.

Equations (29)-(36) are Distflow power flow model commonly used in the distribution network [40]. As Equations (30)-(32) are non-convex constraints, it increases the difficulty of optimization. The second-order cone programming (SOCP) is adopted to convert these complex constraints to convex constraints. The specific relaxation and convexity methods are described as follows [41]–[43].

Define $\tilde{V}_i$ and $\tilde{I}_{ij}$ as follows:

$$\tilde{V}_i = V_i^2. \tag{37}$$

$$\tilde{I}_{ij} = \frac{P_{ij}^2 + Q_{ij}^2}{\tilde{V}_i}. \tag{38}$$

Take these two variables to Equations (30)-(33), we have

$$\sum_{i\in\Omega_{i\to j}} (P_{ij} - r_{ij}\tilde{I}_{ij}) + P_j - g_j\tilde{V}_j = \sum_{k\in\Omega_{j\to k}} P_{jk}. \tag{39}$$

$$\sum_{i\in\Omega_{i\to j}} (Q_{ij} - x_{ij}\tilde{I}_{ij}) + Q_j - b_j\tilde{V}_j = \sum_{k\in\Omega_{j\to k}} Q_{jk}. \tag{40}$$

$$\tilde{V}_j = \tilde{V}_i - 2(r_{ij}P_{ij} + x_{ij}Q_{ij}) + (r_{ij}^2 + x_{ij}^2)\tilde{I}_{ij}. \tag{41}$$

$$V_{i,\min}^2 \leq \tilde{V}_i \leq V_{i,\max}^2. \tag{42}$$

Equation (38) is a non-convex constraint. Its standard format of second-order cone convex can be obtained by SOCP relaxation.

$$\left\| \begin{matrix} 2P_{ij} \\ 2Q_{ij} \\ \tilde{I}_{ij} - \hat{V}_i \end{matrix} \right\|_2 \leq \tilde{I}_{ij} + \tilde{V}_i. \tag{43}$$

By applying SOCP method, the non-convex optimization problem has been transformed into a standard convex optimization problem, which can be solved directly by mature convex optimization algorithms.

Notice that, the proposed ADN dispatching strategy can be conveniently extended to online real time horizon, as in [44], [45]. During online organization, the forecasting information of RES and market price should be updated before each control cycle, and a series of rolling-horizon dispatching commands should be issued to controllable devices timely.

IV. CASE STUDIES

A. GENERATION AND REDUCTION RESULTS OF TYPICAL SCENARIOS

The IEEE 33-bus distribution system is adopted to test the effectiveness and performance of the proposed strategy. The topology of the test is presented in Fig. 3. The cost parameters of distributed generators, energy storage system are given in Table 1 and Table 2. The load curves of each node are derived from the load reference value of IEEE 33 bus system multiplying the actual load demand curve. The capacity for

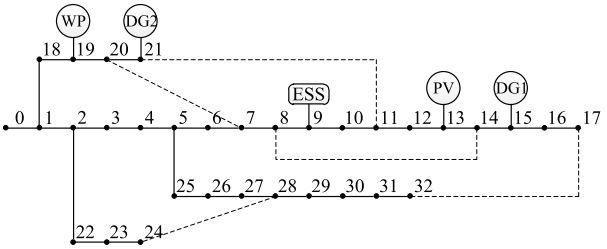

FIGURE 3. IEEE 33-bus distribution system topology.

TABLE 1. Cost parameters of the distributed generators in distribution network.

DG No.	Installed capacity (MW)	Power output (MW)	Ramping (MW/h)	Cost coefficients		
				a_i ($/MWh^2)	b_i ($/MWh)	c_i ($)
#1	2	[1,2]	0.3	1.8	16.2	2.4
#2	2	[1,2]	0.3	2.2	17.5	2.0

TABLE 2. Parameters of the energy storage system in distribution network.

Item	Value	Item	Value
Rated energy capacity	5MWh	Cost coefficient	0.5$/MWh
Rated power capacity	2.5MWh	Dissipation rate	99.0%
Initial energy	1MWh	Conversion rate	95.0%

each branch is set to 2 MW and the voltage security range is set to 0.95∼1.05 p.u.

The forecasted outputs curves of renewable energy resources (RES) are derived from the mean historical curve of Laibin city of China on August, 2019, as in Fig. 4 (a). The wholesale energy market price curve is from the historical clearing locational marginal data issued by PJM on May 6, 2020, as in Fig. 4 (b). The detailed cost and capacity parameters of DGs and ESS are presented in Table 1 and Table 2 respectively. The wind power (WP), Photovoltaic (PV), ESS, DG1 and DG2 are allocated at Bus#19, 13, 9, 15, 21, as in Fig. 3. The uncertainties of RES and market price are assumed to obey the Gaussian distribution. The installation capacities and forecasting error uncertainties parameters of RESs are presented in Table 3.

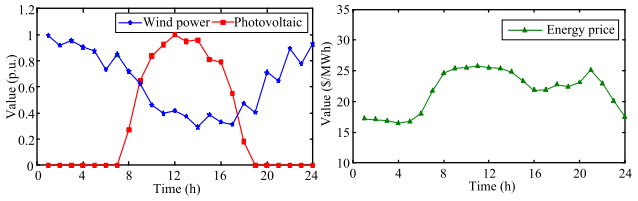

(a). Renewable energy resources forecasting curve.

(b). Wholesale market energy price forecasting curve

FIGURE 4. Hourly forecasting curve of renewable energy resources and wholesale market energy price.

TABLE 3. Uncertainties parameters of RES and market price.

Item	Installation capacity	Forecasting error
Wind power	1MW	10.0%
Photovoltaic	1MW	5.0%
Market price	25.72MWh/$	5.0%

Considering the uncertainties of RESs and market price, 1000 scenarios are generated randomly using Latin hypercube sampling approach, which are named as the original scenario set. After that, the comprehensive similarity measurement method is adopted to compute the similarity between different scenarios. The typical scenario set is

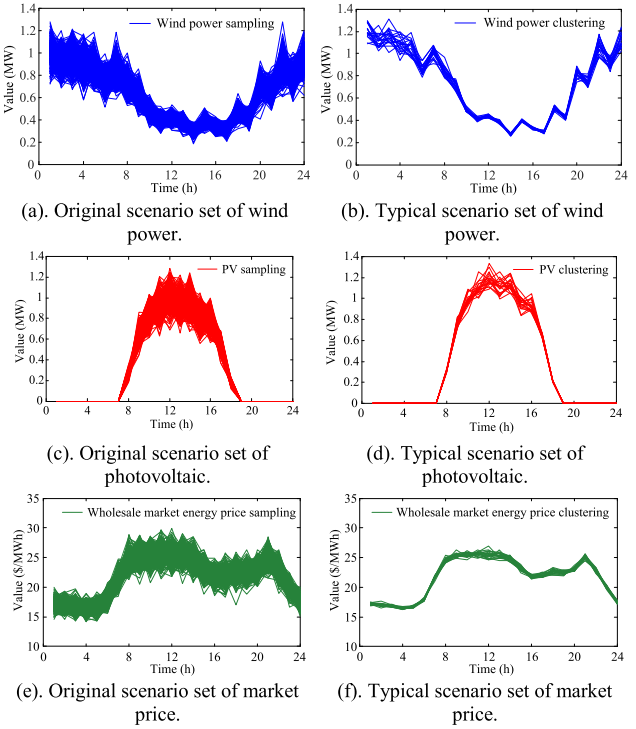

(a). Original scenario set of wind power.

(b). Typical scenario set of wind power.

(c). Original scenario set of photovoltaic.

(d). Typical scenario set of photovoltaic.

(e). Original scenario set of market price.

(f). Typical scenario set of market price.

FIGURE 5. The renewable energy generation curve and wholesale market price curve of the original scenario set and typical scenario set.

TABLE 4. Probabilities of different scenarios in the typical scenario set.

No.	Prob.	No.	Prob.	No.	Prob.	No.	Prob.
#1	8.46%	#6	7.43%	#11	1.17%	#17	2.77%
#2	9.06%	#7	8.34%	#12	2.50%	#17	0.67%
#3	3.30%	#8	9.78%	#13	7.65%	#18	5.11%
#4	5.82%	#9	9.30%	#14	5.11%	#19	1.55%
#5	0.82%	#10	2.96%	#15	6.98%	#20	2.20%

obtained using the proposed graph pyramid based clustering algorithm, as presented in Fig. 5. The probabilities of the scenarios in the typical scenario set are presented in Table 4.

B. OPTIMAL DISPATCH RESULTS OF ADN

According to the typical scenario set obtained by the the proposed clustering algorithm, the ADN optimal dispatch model can provide the day-ahead bidding plans and the optimized operation plans of controllable units. The result comparisons between the original scenario set and typical scenario set are given in Table 5, which indicate that the proposed ADN optimization model with typical scenario set offer a high computational efficiency with a lower operation cost.

The day-ahead bidding plan sent to the superior wholesale energy market is shown in Fig. 6. When the wholesale market price is high, the distribution system operator hopes to sell the energy to the power market. Hence, the generation outputs of distributed generators are adjusted to a relatively high value. Conversely, the VPP prefers to increase energy purchases from the wholesale market and reduce the generation output of generator to save operation cost. The dispatching

TABLE 5. Comparisons of the results obtained using the original scenario set and typical scenario set.

Item	Original scenario set	Typical scenario set	Error (%)
Computational time	543.0 s	11.15 s	--
Final value of objective	974.34$	969.66 $	0.48%
Total DG dispatch	67.32 MWh	66.63 MWh	1.02%
Total ESS dispatch	9.94 MWh	9.75 MWh	1.91%
Expected RES accommodation	21.84 MWh	22.20 MWh	1.65%
Energy sales to the power market	18.38 MWh	18.27 MWh	0.60%

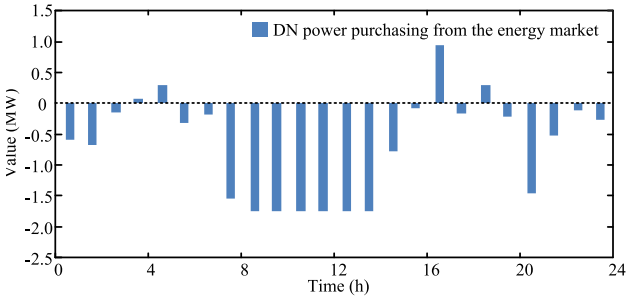

FIGURE 6. The energy bidding plans of the distribution system operator send to the wholesale energy market.

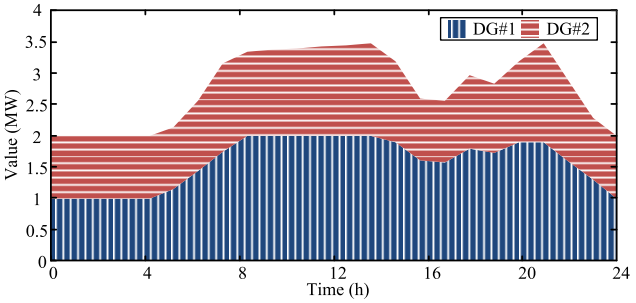

FIGURE 7. Dispatching trajectories of the distribution system operator send to the distributed generators.

trajectories for the distributed generators are presented in Fig. 7. Fig. 8 shows that ESS stores energy when market energy price is low (t = 2-5, 17) and releases its energy when market energy price is high (t = 8-14, 21). It shows that the energy storage system is controlled in an economic manner.

The time-varying voltage variation curves of different nodes are presented in Fig. 9. It shows that the proposed dispatching strategy can ensure the node voltages within the security range (0.95∼1.05). Moreover, the system voltages are greatly influenced by the renewable energy generation since the peak period of voltage and renewable energy resources are highly coincident.

C. PERFORMANCE COMPARISON OF THE PROPOSED STRATEGY

To varify the superiority, the proposed approach is compared with other three methods in terms of economic performance

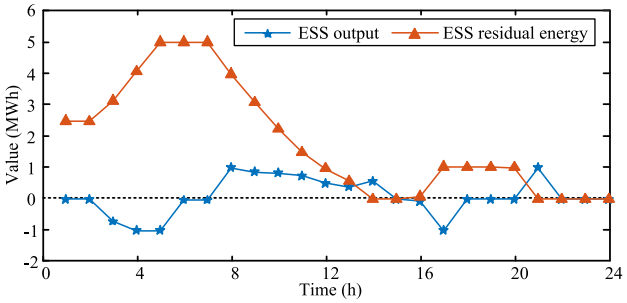

FIGURE 8. Dispatching trajectories of the distribution system operator send to the energy storage system.

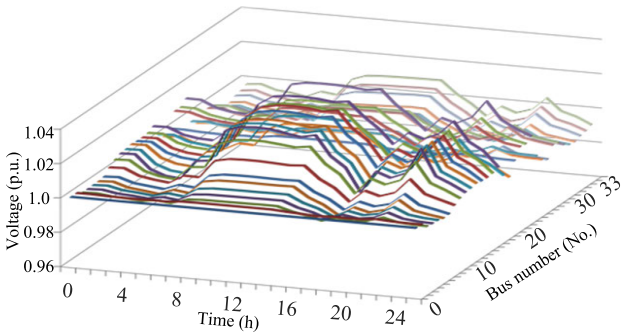

FIGURE 9. Time-varying voltage curves for different nodes in the distribution system.

and computation efficiency. The tests were carried out based on a computer with an Intel i5- 750S CPU. Since the scenario generation process inherents certain randomness, simulations are conducted 50 times and the average computation results in terms of objective function values and computational times are presented Fig. 10 and Fig. 11, respectively. The model features of four different cases are illustrated as follows.

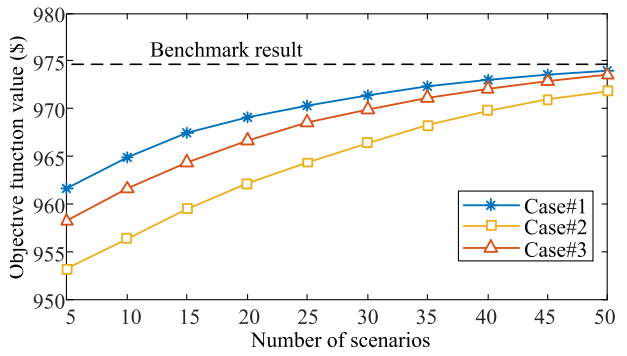

FIGURE 10. Computation results comparisons in terms of objective value.

Case#1: ADN dispatching strategy based on the proposed comprehensive typical scenario set, i.e., the comprehensive typical scenario set is obtained by the proposed scenario generation and reduction method presented in section II.

Case#2: The typical scenario set is only generated by the Latin hypercube sampling method without using the proposed clustering based scenario reduction method.

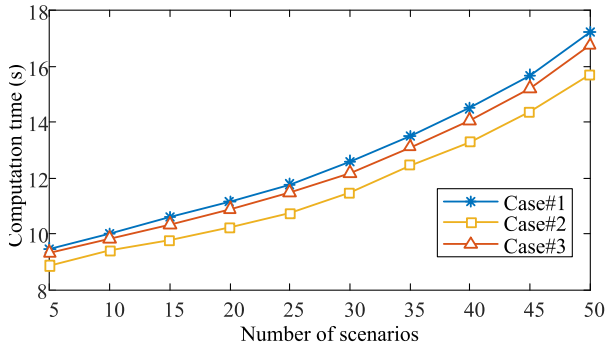

FIGURE 11. Computation results comparisons in terms of computational time.

Case#3: ADN dispatching strategy based on the typical scenarion set generation method proposed in [32]: The scenarios are generated by the Monte Carlo sampling method first, and then reduced by the fast-forward scenario reduction approach based on the Kontorwish distance.

Benchmark: Scenario is generated by the Latin hypercube sampling method and the number of scenario is set to a very large number (1000 in this simulation), which can be regarded as the benchmark to represent the most realistic operational conditions. Table 5 shows the benchmark computation results including the computational time and final objective value calculated under this condition.

Compared with the original scene set, the typical scenario set can save a lot of computing time, as shown in Table 5. However, the overall computational times of the three cases (Case#1-3) using difference scenario generation method are very close, since the computational time is mainly spent on solving the ADN dispatching problem and it takes less time to compute the typical scene set.

Furthermore, it can be indicated from the simulation results that as the number of scenarios increases, the objective function values of Case#1-3 also increase and finally reach to the benchmark value. Therefore, with the increasing of the number of scenarios, stochastic optimization results will tend to be close to the real situation. Moreover, compared with Case#2 and Case#3, the proposed strategy (Case#1) can acheve a more realistic simulation result with comparable computation efficiency.

D. RESULTS ANALYSES UNDER DIFFERENT SYSTEM PARAMETERS

In order to further analyze the influence of different factors on the system economic performance. The proposed ADN dispaching strategy are conducted under different scenarios and the system operation cost are presented in Fig. 12 and Fig. 13. The base values for branch capacity, wholesale market price, RES generation and ESS installation capacity are chosen from subsection 4.1. The simulation parameters of the branch capacity, wholesale market price, RES generation and ESS installation capacity are changed on the basis of the base values. The following conclusions can be drawn according to the simulation results:

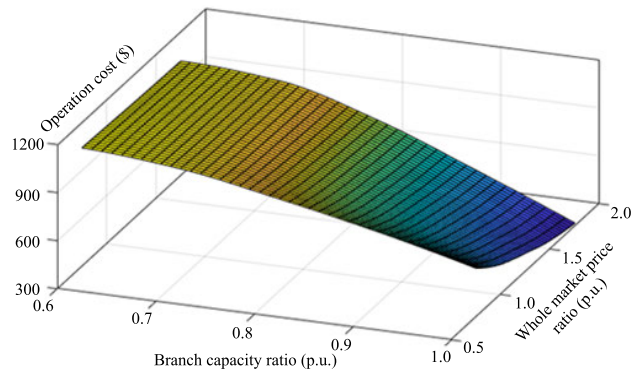

FIGURE 12. System operation cost under different branch capacities and wholesale market prices.

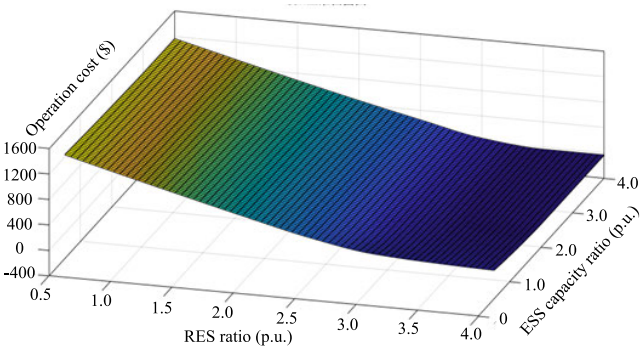

FIGURE 13. System operation cost under different installation capacities of the renewable energy generations and energy storage system.

i). As the wholesale market price increases, the distribution system operator performs as a producer intuitively and gains more profits by selling the energy to the superior energy market.

ii). With the increasing of the branch capacity, the proposed strategy can improve the system operation profit since the congestion limitation is relaxed and the operation flexibility is enlarged. Moreover, the proposed approach can gain more benefit by arbitrage from the power market when the wholesale market price is relatively high. Thus, the ADN dispatching strategy can offers better application effect in the power system with large remaining branch capacity.

iii). The system operation cost can be reduced by promoting the RES penetration level and the ESS capacity, since the system overall flexibility is enhanced by increasing these parameters. Nevertheless, subjected to branch congestions and voltage limitation, the system operation cost will decrease to a limit value eventually.

V. CONCLUSION

This study proposes a comprehensive typical scenario set based stochastic economic dispatching strategy for the active distribution network. The proposed method can provide the day-ahead bidding plan to the wholesale market and the dispatching plan to the controllable units, which can the DSO

perform as prosumers when participating in the wholesale market operation. Compared with typical scenario formulation methods as in [31]–[32], the proposed comprehensive typical scenario set consider multiple similarity measurement indexes, which can model the uncertainties more reasonably and improve the computational efficiency effectively. The effectiveness and scalability of proposed approach is verified under different implementation scenarios based on the IEEE 33-bus distribution system, which illustrates that the proposed approach owns high computational efficiency and promotes the security and economy of the distribution system operation.

Furthermore, as the penetration of distributed energy resources increases, the flexibility of ADN will be improved considerably in the future and can be used to provide the ancillary services. Therefore, the operation strategy of ADN providing multiple services for the power market under uncertain environments is a promising research direction in future works.

REFERENCES

[1] N. Karthikeyan, J. R. Pillai, B. Bak-Jensen, and J. W. Simpson-Porco, "Predictive control of flexible resources for demand response in active distribution networks," *IEEE Trans. Power Syst.*, vol. 34, no. 4, pp. 2957–2969, Jul. 2019.

[2] R. Li, W. Wang, and M. Xia, "Cooperative planning of active distribution system with renewable energy sources and energy storage systems," *IEEE Access*, vol. 6, pp. 5916–5926, 2018, doi: 10.1109/ACCESS.2017.2785263.

[3] H. Yuan, F. Li, Y. Wei, and J. Zhu, "Novel linearized power flow and linearized OPF models for active distribution networks with application in distribution LMP," *IEEE Trans. Smart Grid*, vol. 9, no. 1, pp. 438–448, Jan. 2018.

[4] W. Wei, J. Wang, and L. Wu, "Distribution optimal power flow with real-time price elasticity," *IEEE Trans. Power Syst.*, vol. 33, no. 1, pp. 1097–1098, Jan. 2018.

[5] M. Usman, A. Cervi, M. Coppo, F. Bignucolo, and R. Turri, "Cheap conic OPF models for low-voltage active distribution networks," *IEEE Access*, vol. 8, pp. 99691–99708, 2020, doi: 10.1109/ACCESS.2020.2998054.

[6] Z. Li, W. Wu, and B. Zhang, "A large-scale reactive power optimization method based on Gaussian penalty function with discrete control variables," *Proc. CSEE*, vol. 33, no. 4, pp. 68–76, Feb. 2013.

[7] T. Ding, Q. Guo, and R. Bo, "A two-stage heuristic-correction for dynamic reactive power optimization based on relaxation-MPEC and MIQP," *Proc. CSEE*, vol. 34, no. 13, pp. 2100–2107, May 2014.

[8] Y. Cheng and M. Liu, "Nonlinear primal-dual interior point algorithm for discrete reactive power optimization," *Autom. Electr. Power Syst.*, vol. 25, no. 9, pp. 23–27, 2001.

[9] Y. Cheng and M. Liu, "Reactive power optimization of large-scale power systems with discrete control variables," *Proc. CSEE*, vol. 22, no. 5, pp. 55–61, May 2002.

[10] Y.-C. Wu, A. S. Debs, and R. E. Marsten, "A direct nonlinear predictor-corrector primal-dual interior point algorithm for optimal power flows," *IEEE Trans. Power Syst.*, vol. 9, no. 2, pp. 876–883, May 1994.

[11] J. Zhao, L. Ju, Z. Dai, and G. Chen, "Voltage stability constrained dynamic optimal reactive power flow based on branch-bound and primal–dual interior point method," *Int. J. Electr. Power Energy Syst.*, vol. 73, pp. 601–607, Dec. 2015.

[12] C. Wu, P. Jiang, Y. Sun, C. Zhang, and W. Gu, "Economic dispatch with CHP and wind power using probabilistic sequence theory and hybrid heuristic algorithm," *J. Renew. Sustain. Energy*, vol. 9, no. 1, pp. 1–16, 2017.

[13] A. G. Bakirtzis, P. N. Biskas, C. E. Zoumas, and V. Petridis, "Optimal power flow by enhanced genetic algorithm," *IEEE Trans. Power Syst.*, vol. 17, no. 2, pp. 229–236, May 2002.

[14] P. Acharjee and S. K. Goswami, "A decoupled power flow algorithm using particle swarm optimization technique," *Energy Convers. Manage.*, vol. 50, no. 9, pp. 2351–2360, Sep. 2009.

[15] P. E. O. Yumbla, J. M. Ramirez, and C. A. C. Coello, "Optimal power flow subject to security constraints solved with a particle swarm optimizer," *IEEE Trans. Power Syst.*, vol. 23, no. 1, pp. 33–40, Feb. 2008.

[16] E. Oh and H. Wang, "Reinforcement-learning-based energy storage system operation strategies to manage wind power forecast uncertainty," *IEEE Access*, vol. 8, pp. 20965–20976, 2020.

[17] C. Chen, M. Cui, F. F. Li, S. Yin, and X. Wang, "Model-free emergency frequency control based on reinforcement learning," *IEEE Trans. Ind. Informat.*, early access, Jun. 9, 2020, doi: 10.1109/TII.2020.3001095.

[18] Z. Li, L. Ye, Y. Zhao, X. Song, J. Teng, and J. Jin, "Short-term wind power prediction based on extreme learning machine with error correction," *Protection Control Modern Power Syst.*, vol. 1, no. 1, pp. 9–16, Dec. 2016.

[19] J. Lavaei and S. H. Low, "Zero duality gap in optimal power flow problem," *IEEE Trans. Power Syst.*, vol. 27, no. 1, pp. 92–107, Feb. 2012.

[20] Y. Liu, W. Wu, and B. Zhang, "A mixed integer second-order cone programming based active and reactive power coordinated multi-period optimization for active distribution network," *Proc. CSEE*, vol. 34, no. 16, pp. 2575–2583, Jun. 2014.

[21] Y. Li, H. Zhang, X. Liang, and B. Huang, "Event-triggered-based distributed cooperative energy management for multienergy systems," *IEEE Trans. Ind. Informat.*, vol. 15, no. 4, pp. 2008–2022, Apr. 2019.

[22] C. Wu, W. Gu, P. Jiang, Z. Li, H. Cai, and B. Li, "Combined economic dispatch considering the time-delay of district heating network and multi-regional indoor temperature control," *IEEE Trans. Sustain. Energy*, vol. 9, no. 1, pp. 118–127, Jan. 2018.

[23] X. Bai, L. Qu, and W. Qiao, "Robust AC optimal power flow for power networks with wind power generation," *IEEE Trans. Power Syst.*, vol. 31, no. 5, pp. 4163–4164, Sep. 2016.

[24] F. Alismail, P. Xiong, and C. Singh, "Optimal wind farm allocation in multi-area power systems using distributionally robust optimization approach," *IEEE Trans. Power Syst.*, vol. 33, no. 1, pp. 536–544, Jan. 2018.

[25] S. Choi and S. Kim, "An investigation of operating behavior characteristics of a wind power system using a fuzzy clustering method," *Expert Syst. Appl.*, vol. 81, pp. 244–250, Sep. 2017.

[26] Y. Hao, L. Dong, X. Liao, J. Liang, L. Wang, and B. Wang, "A novel clustering algorithm based on mathematical morphology for wind power generation prediction," *Renew. Energy*, vol. 136, pp. 572–585, Jun. 2019.

[27] Z. Li, W. Wu, B. Zhang, and B. Wang, "Adjustable robust real-time power dispatch with large-scale wind power integration," *IEEE Trans. Sustain. Energy*, vol. 6, no. 2, pp. 357–368, Apr. 2015.

[28] X. Su, X. Bai, X. Liu, R. Zhu, and C. Wei, "Research on robust stochastic dynamic economic dispatch model considering the uncertainty of wind power," *IEEE Access*, vol. 6, pp. 357–368, 2015.

[29] W. Wu, J. Chen, B. Zhang, and H. Sun, "A robust wind power optimization method for look-ahead power dispatch," *IEEE Trans. Sustain. Energy*, vol. 5, no. 2, pp. 507–515, Apr. 2014.

[30] Z. Yi, Y. Xu, J. Zhou, W. Wu, and H. Sun, "Bi-level programming for optimal operation of an active distribution network with multiple virtual power plants," *IEEE Trans. Sustain. Energy*, vol. 11, no. 4, pp. 2855–2869, Oct. 2020.

[31] N. Gupta, "Stochastic optimal reactive power planning and active power dispatch with large penetration of wind generation," *J. Renew. Sustain. Energy*, vol. 10, no. 2, Mar. 2018, Art. no. 025902.

[32] S. Bahramara, M. Yazdani-Damavandi, J. Contreras, M. Shafie-Khah, J. P. S. Catalão, "Modeling the strategic behavior of a distribution company in wholesale energy and reserve markets," *IEEE Trans. Smart Grid*, vol. 9, no. 4, pp. 3857–3870, Jul. 2018.

[33] Z. Yi, Y. Xu, W. Gu, and W. Wu, "A multi-time-scale economic scheduling strategy for virtual power plant based on deferrable loads aggregation and disaggregation," *IEEE Trans. Sustain. Energy*, vol. 11, no. 3, pp. 1332–1346, Jul. 2020.

[34] M. Ali, I.-S. Ilie, J. V. Milanovic, and G. Chicco, "Wind farm model aggregation using probabilistic clustering," *IEEE Trans. Power Syst.*, vol. 28, no. 1, pp. 309–316, Feb. 2013.

[35] S. Yang, C. Li, X. Li, Y. Huang, C. Liu, and W. Wang, "Wind power fluctuation characteristics of three north regions based on clustering algorithm," *J. Eng.*, vol. 2017, no. 13, pp. 2266–2270, Jan. 2017.

[36] Z. Shu and P. Jirutitijaroen, "Latin hypercube sampling techniques for power systems reliability analysis with renewable energy sources," *IEEE Trans. Power Syst.*, vol. 26, no. 4, pp. 2066–2073, Mar. 2011.

[37] S. Lin, F. Li, E. Tian, Y. Fu, and D. Li, "Clustering load profiles for demand response applications," *IEEE Trans. Smart Grid*, vol. 10, no. 2, pp. 1599–1607, Mar. 2019.
[38] X. Lv, Y. Ma, X. Zhang, S. Li, and Y. Zhang, "A clustering algorithm based on graph pyramid," *Comput. Appliance Softw.*, vol. 35, no. 2, pp. 256–261, 2018.
[39] Q. Li and V. Vittal, "Non-iterative enhanced SDP relaxations for optimal scheduling of distributed energy storage in distribution systems," *IEEE Trans. Power Syst.*, vol. 32, no. 3, pp. 1721–1732, May 2017.
[40] C. Lin, W. Wu, X. Chen, and W. Zheng, "Decentralized dynamic economic dispatch for integrated transmission and active distribution networks using multi-parametric programming," *IEEE Trans. Smart Grid*, vol. 9, no. 5, pp. 4983–4993, Sep. 2018.
[41] W. Zheng, W. Wu, B. Zhang, H. Sun, and Y. Liu, "A fully distributed reactive power optimization and control method for active distribution networks," *IEEE Trans. Smart Grid*, vol. 7, no. 2, pp. 1021–1033, Mar. 2016.
[42] L. Yang, Y. Xu, H. Sun, and X. Zhao, "Two-stage convexification-based optimal electricity-gas flow," *IEEE Trans. Smart Grid*, vol. 11, no. 2, pp. 1465–1475, Mar. 2020.
[43] M. E. Baran and F. F. Wu, "Network reconfiguration in distribution systems for loss reduction and load balancing," *IEEE Trans. Power Del.*, vol. 4, no. 2, pp. 1401–1407, Apr. 1989.
[44] M. Forghani and S. Afsharnia, "Online wavelet transform-based control strategy for UPQC control system," *IEEE Trans. Power Del.*, vol. 22, no. 1, pp. 481–491, Jan. 2007.
[45] S. Fan, G. He, X. Zhou, and M. Cui, "Online optimization for networked distributed energy resources with time-coupling constraints," *IEEE Trans. Smart Grid*, early access, Jul. 21, 2020, doi: 10.1109/TSG.2020.3010866.

HUIMIN ZHU (Student Member, IEEE) was born in 1982. She is currently pursuing the Ph.D. degree in power system operation and control with the School of Electrical Engineering, Shenyang University of Technology, Shenyang. Her current research interests include the modeling and control methods of virtual synchronous photovoltaic power station.

SHUN YUAN (Member, IEEE) was born in 1963. He is currently a Ph.D. Supervisor with the School of Electrical Engineering, Shenyang University of Technology, Shenyang. He is majoring in power system operation and control.

CHUNLAI LI (Member, IEEE) was born in 1980. He is currently pursuing the Ph.D. degree with the School of Electrical Engineering, Shenyang University of Technology, Shenyang. He is majoring in power system operation and control. His current research interests include the parameter identification and stability control method of photovoltaic grid-connected systems.